PCCP

PAPER

View Article Online
View Journal | View Issue

Cite this: *Phys. Chem. Chem. Phys.*, 2026, **28**, 5175

A simple approach to attosecond electronic chirality flips using triatomic molecules

Dietrich Haase,[a] Jörn Manz,*[a] Beate Paulus,[a] Jonathan Scherlitzki[a] and Jean Christophe Tremblay*[b]

Received 28th November 2025,
Accepted 29th January 2026

DOI: 10.1039/d5cp04637h

rsc.li/pccp

Electronic chirality flips in achiral molecules is a hot topic in attosecond and femtosecond chemistry and physics. Our quantum dynamics simulations show that this effect can be induced by a simple Franck–Condon excitation of the $A' + A''$ superposition of the electronic A' ground state plus the first excited A'' state in the oriented bent triatomic heteronuclear molecule NSF.

I. Introduction

Chiral molecules, that is, molecules with chiral nuclear frames, have chiral electronic densities in their stationary electronic eigenstates, with rare exceptions.[1] Accordingly, opposite R and S enantiomers have electronic densities with opposite chiralities. This is obviously the case for *all* their stationary electronic eigenstates. In contrast, it came as a complete surprise that femtosecond (fs) laser pulses can prepare superpositions of electronic eigenstates which induce electronic chirality flips in chiral molecules.[2] Those flips occur on the time scale of a few fs, and they can be monitored, *e.g.*, by time-resolved photoelectron dichroism.[2,3] This discovery stimulated two extensions, namely quantum dynamics simulations of fs-laser-induced electronic chirality flips even in oriented achiral molecules, and even in the time domain of a few hundred attoseconds (as), specifically in oriented NaK[4] and RbCs.[5] Meanwhile, the phenomenon of electronic chirality flips in achiral molecules has been confirmed in another theoretical work, with application to oriented furan.[6]

The key to these phenomena in achiral molecules[4–6] is the fact that fs laser pulses can prepare electronic superposition states which break electronic symmetry without breaking nuclear symmetry.[7,8] This effect may last for a few fs, when the nuclei are practically frozen. In extreme cases, the laser pulses can even break all electronic symmetries. Consequently, the electronic density of the corresponding superposition states is chiral even though the constituting electronic eigenstates and the nuclear frame are achiral. However, breaking all electronic symmetries is quite a challenge if the underlying nuclear frame has many symmetry elements. For example, the nuclear frames and the electronic eigenstates of heteronuclear diatomic molecules such as NaK[4] or RbCs[5] have $C_{\infty v}$ symmetry with an infinite number of symmetry elements. Amazingly, these can be broken by a well-designed set of two circularly polarized laser pulses.[4,5]

By comparison with the pioneering references,[4,5] this work presents quantum dynamics simulations of a much simpler realization of laser-induced electronic chirality flips in an achiral molecule. For this purpose, we consider a bent triatomic heteronuclear molecule, specifically oriented thiazyl fluoride (NSF), a key substance in sulfur–nitrogen–fluorine chemistry.[9] Its nuclear frame and consequently the electronic eigenstates have C_s symmetry, *i.e.*, they possess only one symmetry element, the symmetry plane σ, in addition to the omnipresent identity E. It is easy to predict that breaking the single symmetry element σ of the electronic densities of eigenstates in NSF should be much easier than breaking the corresponding infinite number of symmetry elements of NaK or RbCs. Specifically, we shall show that a simple Franck–Condon (FC) excitation from the electronic ground state A' to the first excited eigenstate A'' can prepare an electronic superposition state ψ which does not possess any mirror plane, or in other words: preparation of ψ breaks C_s symmetry. Hence, ψ must be chiral, and since it is not an eigenstate, it is time-dependent and induces electronic chirality flips.

II. Model and methods

We assume that the achiral bent NSF molecule with C_s symmetry has been pre-oriented such that the body-fixed molecular plane corresponds to the xy-plane of the laboratory frame, as shown in Fig. 1. This can be achieved by means of z-polarized THz and femtosecond laser pulses.[10] Alternatively, orientation can also be achieved experimentally using static electric fields[11,12] or by

[a] *Institut für Chemie und Biochemie, Freie Universität Berlin, 14195 Berlin, Germany. E-mail: jmanz@chemie.fu-berlin.de*
[b] *CNRS-Université de Lorraine, LPCT, 57070 Metz, France. E-mail: jean-christophe.tremblay@univ-lorraine.f*

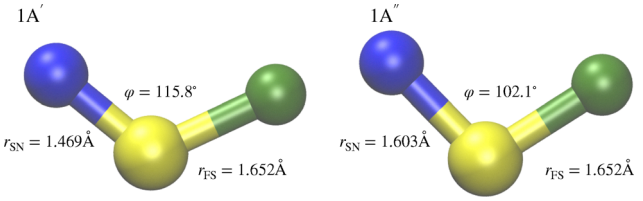

Fig. 1 Geometries of NSF in the electronic ground state A' and in the first excited state A'', oriented in the xy-plane. Fluorine in green, sulfur in yellow, nitrogen in blue.

creation of a long-lived rotational wave packet with field-free orientational recurrences.[13]

Quantum chemical calculations—performed using the Molpro[14] implementation of the (1,2)-SA-CASSCF/SS-CASSCF method[15–17] with an aug-cc-pVTZ basis set[18] on all atoms—yield the electronic eigenfunctions of the ground and excited states, respectively labeled $\psi_{A'}(\mathbf{x};\mathbf{Q})$ and $\psi_{A''}(\mathbf{x};\mathbf{Q})$. They depend on the N electronic coordinates $\boldsymbol{x} = \{\boldsymbol{r}_1, \varsigma_1, \boldsymbol{r}_2, \varsigma_2, \ldots, \boldsymbol{r}_N, \varsigma_N\}$, where $\boldsymbol{r}_i$ is the position of the electron and ς_i is its spin, and (parametrically) on all nuclear coordinates, $\mathbf{Q}$. Varying the nuclear configuration yields the potential energy surfaces (PESs) $V_{A'}(\mathbf{Q})$ and $V_{A''}(\mathbf{Q})$ associated with NSF in the electronic ground and first excited states. The corresponding irreducible representations are A' and A'', *cf.* the character table of C_s symmetry in Table 1; here the notation σ is also used for reflection at NSF's mirror plane. As only singlet states of NSF are considered, the effect of spin–orbit coupling is assumed to be negligible for electronic excitations.

Accordingly, reflection σ at NSF's mirror plane yields

$$\sigma\psi_{A'}(\mathbf{x};\mathbf{Q}) = \psi_{A'}(\mathbf{x};\mathbf{Q}), \tag{1}$$

$$\sigma\psi_{A''}(\mathbf{x};\mathbf{Q}) = -\psi_{A''}(\mathbf{x};\mathbf{Q}). \tag{2}$$

The PESs $V_{A'}(\mathbf{Q})$ and $V_{A''}(\mathbf{Q})$ have potential minima at $\mathbf{Q}_{\mathrm{m},A'}$ and $\mathbf{Q}_{\mathrm{m},A''}$, with associated geometries as shown in Fig. 1 and with corresponding vibrational frequencies. For convenience, the energy of the potential minimum of the ground state is set to zero,

$$V_{A'}(\mathbf{Q}_{\mathrm{m},A'}) = 0.$$

The nuclear wavefunction $\chi_{A',0}(\mathbf{Q})$ of the vibrational ground state embedded in the ground electronic PES $V_{A'}(\mathbf{Q})$ represents the lowest vibronic state of the system. In the present work, it is computed by imaginary time propagation of a full-dimensional nuclear wave packet on the ground electronic PES using the Heidelberg implementation of the Multi-Configuration Time-Dependent Hartree (MCTDH) method, as described in ref. 19.

We assume that the molecule is prepared in the superposition state

$$\psi(\mathbf{x};\mathbf{Q}_{\mathrm{m},A'}) = c_{A'}e^{i\delta_{A'}}\psi_{A'}(\mathbf{x};\mathbf{Q}_{\mathrm{m},A'}) + c_{A''}e^{i\delta_{A''}}\psi_{A''}(\mathbf{x};\mathbf{Q}_{\mathrm{m},A'}) \tag{3}$$

Table 1 Character table for C_s symmetry

C_s	E	σ
A'	1	1
A''	1	−1

with real-valued, positive amplitudes $c_{A'}$, $c_{A''}$ and phases $\delta_{A'}$, $\delta_{A''}$, by means of Franck–Condon (FC) excitation with the nuclei frozen at $\mathbf{Q}_{\mathrm{m},A'}$ using a linearly z polarized laser. The preparation of the superposition state determines the initial values of the relative phase. The results discussed below are primarily obtained from the analytical two-level model at frozen nuclear geometry. Nuclear wavepacket calculations were used only as a complementary check to ensure that the excited-state coherence remains close to unity for about 1 fs, and not to extract electronic densities. Accordingly, the densities discussed should not be interpreted as arising from a propagated molecular wavepacket at $\mathbf{Q} = \mathbf{Q}_{\mathrm{m},A'}$.

Neglecting diabatic transitions, the corresponding electronic populations are

$$P_{A'} = {c_{A'}}^2, \quad P_{A''} = {c_{A''}}^2. \tag{4}$$

The vertical excitation energy is

$$\Delta E = V_{A''}(\mathbf{Q}_{\mathrm{m},A'}) - V_{A'}(\mathbf{Q}_{\mathrm{m},A'}) \equiv \hbar\omega \tag{5}$$

with corresponding resonant frequency ω. Subsequently, the superposition state evolves as

$$\psi(\mathbf{x},\mathrm{t};\mathbf{Q}_{\mathrm{m},A'}) = c_{A'}e^{i\delta_{A'}}\psi_{A'}(\mathbf{x};\mathbf{Q}_{\mathrm{m},A'}) + c_{A''}e^{i\delta_{A''}}\psi_{A''}(\mathbf{x};\mathbf{Q}_{\mathrm{m},A''})e^{-i\omega t}, \tag{6}$$

or in Dirac notation,

$$|\psi(t)\rangle = c_{A'}e^{i\delta_{A'}}|\psi_{A'}\rangle + c_{A''}e^{i\delta_{A''}}|\psi_{A''}\rangle e^{-i\omega t}. \tag{7}$$

The corresponding one-electron density of the electrons at position $\boldsymbol{r}$ is obtained as the expectation value of the density operator, $\hat{\rho}(\mathbf{r}) = \sum_k \delta(\mathbf{r}_k - \mathbf{r})$, over the wave packet. It evolves in time as

$$\begin{aligned}\rho(\mathbf{r},t) &= \left\langle \psi(t)\middle|\sum_k \delta(\mathbf{r}_k-\mathbf{r})\middle|\psi(t)\right\rangle \\ &= P_{A'}\rho_{A'}(\mathbf{r}) + P_{A''}\rho_{A''}(\mathbf{r}) \\ &\quad + 2c_{A'}c_{A''}\cos(\delta_{A'}-\delta_{A''}+\omega t)\rho_{A'A''}(\mathbf{r}),\end{aligned} \tag{8}$$

where

$$\rho_{A'}(r) = \left\langle \psi_{A'}\middle|\sum_k \delta(\mathbf{r}_k-\mathbf{r})\middle|\psi_{A'}\right\rangle, \tag{9}$$

$$\rho_{A''}(\mathbf{r}) = \left\langle \psi_{A''}\middle|\sum_k \delta(\mathbf{r}_k-\mathbf{r})\middle|\psi_{A''}\right\rangle, \tag{10}$$

$$\rho_{A'A''}(\mathbf{r}) = \left\langle \psi_{A'}\middle|\sum_k \delta(\mathbf{r}_k-\mathbf{r})\middle|\psi_{A''}\right\rangle, \tag{11}$$

These densities are computed by analytical integration of the N-electron wave packet over all electrons and spin degrees of freedom using ORBKIT.[20,21]

The expression for the time evolution of the electronic density is an approximation that depends on electronic coherence in the ground and excited states. This coherence can be measured by the overlap

$$S_{A',A''}(t) = \langle\chi_{A'}(\mathbf{Q},t)|\chi_{A''}(\mathbf{Q},t)\rangle \tag{12}$$

of the corresponding nuclear wavefunctions in the A' and A'' states.[22,23] Good overlap, $|S_{A',A''}(t)| \approx 1$, implies satisfactory electronic coherence.

Evaluations of $S_{A'A''}(t)$ require calculations of $\chi_{A'}(\mathbf{Q},t)$ and $\chi_{A''}(\mathbf{Q},t)$. Using the FC excitation picture, the initial nuclear wavefunction in the excited state is

$$\chi_{A''}(\mathbf{Q},0) = \chi_{A',0}(\mathbf{Q}) \tag{13}$$

Subsequently, $\chi_{A''}(\mathbf{Q},t)$ evolves on the PES $V_{A''}(\mathbf{Q})$ starting from this initial condition. The nuclear quantum dynamics of $\chi_{A''}(\mathbf{Q},t)$ is evaluated using the MCTDH method.[19,24] For this purpose, the potential energy surface $V_{A''}(\mathbf{Q})$ is adjusted using the PotFit algorithm implemented in the Heidelberg package.[19] More details on the dynamical simulations can be found in the SI, section S3.

We assume that the nuclear wavefunction in the ground state remains robust,

$$\chi_{A'}(\mathbf{Q},t) = \chi_{A',0}(\mathbf{Q}), \tag{14}$$

neglecting subsequent effects of $A' \rightarrow A''$ ground state vibrational coherence induced by impulsive absorption.[25] Consequently, the nuclear overlap is approximated as the autocorrelation function of the nuclear wavefunction in the excited state,

$$S_{A'A''}(t) \approx \langle \chi_{A',0}(\mathbf{Q})|\chi_{A''}(\mathbf{Q},t)\rangle = \langle \chi_{A''}(\mathbf{Q},0)|\chi_{A''}(\mathbf{Q},t)\rangle, \tag{15}$$

In the following, we consider the scenario where the FC transition transfers half of the population of the ground state to the excited state,

$$P_{A'} = P_{A''} = \frac{1}{2}.$$

The corresponding amplitudes and phases are

$$c_{A'} = c_{A''} = \frac{1}{\sqrt{2}}, \quad \delta_{A'} = \delta_{A''} = 0. \tag{16}$$

The subsequent results are robust with respect to different scenarios, *e.g.*, less efficient population transfer or non-zero phases. In previous work on oriented benzene, we have shown that short laser pulses can be used to tailor the same initial electron density, but that ensuing field-free charge migration is critically influenced by the relative phase accumulated during the laser excitation.[26]

III. Results and discussion

The quantum chemical results for the time-independent nuclear properties of NSF in the ground (A') and first excited (A'') states are documented in Section S1 of the SI. Accordingly, the potential minimum on the excited electronic state $\mathbf{Q}_{\mathrm{m},A''}$ is shifted relative to that of the ground electronic state $\mathbf{Q}_{\mathrm{m},A'}$, as can be seen from the geometries reported in Fig. 1. Despite their similarities, with geometries and vibrational frequencies that correlate well with each other, they are not strictly identical. The consequences will be discussed below.

For the present investigation, the most important property of the superposition state $\psi(\mathbf{x},t;\ \mathbf{Q}_{\mathrm{m},A'})$ is that it is not an eigenstate of reflection at the nuclear mirror plane,

$$\sigma\psi(\mathbf{x},t;\ \mathbf{Q}_{\mathrm{m},A'}) \neq \pm\psi(\mathbf{x},t;\ \mathbf{Q}_{\mathrm{m},A'}), \tag{17}$$

even though the constituting electronic eigenfunctions *are* eigenstates of σ (*cf.* eqn (1) and (2) in Section II). This means that Franck–Condon (FC) preparation of the superposition state $\psi(\mathbf{x},t;\ \mathbf{Q}_{\mathrm{m},A'})$ effectively breaks the C_s symmetry imposed by the nuclear frame.

This result is also obtained directly from the character table (Table 1), *cf.* ref. 8 the two constituents of $\psi(\mathbf{x},t;\ \mathbf{Q}_{\mathrm{m},A'})$ have irreducible representations A' and A''. The only symmetry element common to A' and A'' is the identity E. Hence, the symmetry of the superposition state $\psi(\mathbf{x},t;\ \mathbf{Q}_{\mathrm{m},A'})$ is C_1 instead of C_s. Consequently, $\psi(\mathbf{x},t;\ \mathbf{Q}_{\mathrm{m},A'})$ is *chiral*, although the nuclei still transform according to the C_s point group. The derivation in ref. 8 shows that if $\psi(\mathbf{x},t;\ \mathbf{Q}_{\mathrm{m},A'})$ is chiral, then its one-electron density $\rho(\boldsymbol{r},t)$ is also chiral, except at the rare times when its time-dependent part vanishes, *i.e.* when

$$\cos(\delta_{A'} - \delta_{A''} + \omega t) = 0 \tag{18}$$

in eqn (8).

To document the chirality of the electronic density $\rho(\boldsymbol{r},t)$ of the superposition state $\psi(\mathbf{x},t;\ \mathbf{Q}_{\mathrm{m},A'})$, we focus on its time-dependent part, divided by the scaling factor $2c_{A'}c_{A''}$ (equal to 1 in the present scenario). Thus, we analyze the universal term

$$\cos(\delta_{A'} - \delta_{A''} + \omega t)\rho_{A'A''}(\boldsymbol{r}) \tag{19}$$

which appears in all $A' \rightarrow A''$ FC transitions of NSF (with possibly different phase shifts).

The electronic density is periodic, with period

$$\tau = \frac{2\pi}{\omega} = \frac{h}{\Delta E}.$$

In the present case, $\Delta E = 3.745$ eV, $\omega = 5.689$ rad fs^{-1}, hence $\tau = 1.104$ fs. The time evolution of $\cos(\delta_{A'} - \delta_{A''} + \omega t)\rho_{A'A''}$ with phase shift $\delta_{A'} - \delta_{A''} = 0$ is shown by the snapshots in Fig. 2 for the first period, $0 \leq t \leq \tau$ (see panels labeled a) for an in-plane view, and panels labeled b) for the top view).

Apparently, the electron density is always chiral except at the special time over the first half period

$$t_1 = \frac{\tau}{4} = 276 \text{ as},$$

when $\cos(\omega t) = \cos(\pi/2) = 0$. Furthermore, inspection of the snapshots shows that the densities at $t_1 - t$ and $t_1 + t$ are enantiomers. That is, the chirality of $\rho(\boldsymbol{r},t)$ flips at t_1. Equivalent chirality flips occur at

$$t_2, t_3, t_4, \ldots = \frac{3\tau}{4}, \frac{5\tau}{4}, \frac{7\tau}{4}, \ldots$$

The series of snapshots in Fig. 2a and b also shows that the amplitude of the time-dependent term $\cos(\delta_{A'} - \delta_{A''} + \omega t)\rho_{A'A''}$ varies periodically, but the *shape* of $\rho_{A'A''}$ remains invariant. Note that the results are obtained for a 1 : 1 superposition state

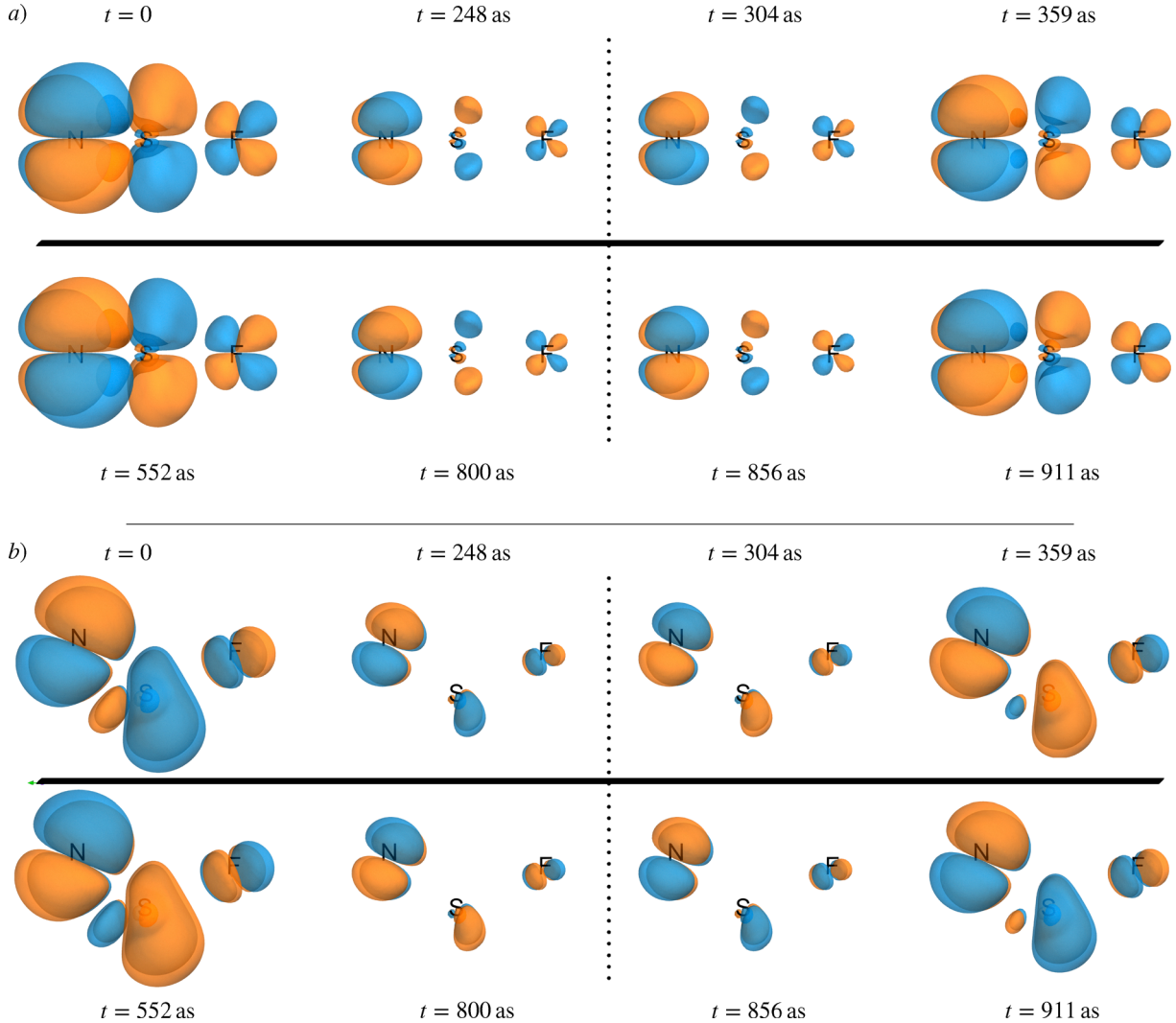

Fig. 2 Attosecond charge migration in the $A' + A''$ superposition state of NSF. The time-evolution of the wave packet is documented by the universal transition density component, eqn (19), of the one-electron density, eqn (8). (a) in-plane view, with S pointing away from the reader; (b) top view, as in Fig. 1. The respective upper/lower panels show selected snapshots during the first/second half period of charge migration. The vertical dashed line marks the time at which chirality flips occur. In panels (a), the horizontal solid line emphasizes the mirror symmetry of the transition density over the two half-periods. Positive/negative isocontours at $\pm 0.0025/a_0^3$ in orange/blue.

in a two-level systems, but they would be valid for different excitation scenarios, *e.g.*, less efficient population transfer or non-zero phases.

To provide a quantitative measure of the magnitude of this effect, we choose to investigate the expectation value of the out-of-plane coordinate, z, as a function of time. It documents the asymmetry with respect to the molecular plane and the degree of chirality. The results are shown in Fig. 3. In the optimal scenario studied here, the magnitude of the induced chirality is found to be small. Yet, it is likely to be sufficiently large to be observed experimentally *via* the variation of the electric dipole perpendicular to the molecular plane.

The rather complex shape of the transition density is well approximated by the simple expression

$$\rho_{A'A''}(\mathbf{r}) \approx \sqrt{2}\phi_{\mathrm{HOMO}}(\mathbf{r};\mathbf{Q}_{A'})\phi_{\mathrm{LUMO}}(\mathbf{r};\mathbf{Q}_{A'}), \qquad (20)$$

where $\phi_{\mathrm{HOMO}}(\boldsymbol{r};\mathbf{Q}_{A'})$ and $\phi_{\mathrm{LUMO}}(\boldsymbol{r};\mathbf{Q}_{A'})$ are the highest occupied and lowest unoccupied molecular orbitals of the dominant-determinant approximation to the electronic ground state A'. This relation, illustrated in Fig. 4, confirms that the $A' \rightarrow A''$ FC excitation of NSF is essentially a HOMO $\rightarrow$ LUMO transition. The derivation is provided in Section S2.

As explained in Section II, eqn (8) for the electronic density $\rho(\boldsymbol{r},t)$ is an approximation that relies on electronic coherence in the $A' + A''$ superposition state. A criterion for the validity of this approximation is that the magnitude of the autocorrelation function, $|S_{A'A''}(t)|$, should remain close to 1. To investigate this, we calculate $|S_{A'A''}(t)|$ as outlined in Section II. The result is shown in Fig. 5. Apparently, $|S_{A'A''}(t)|$ decays rapidly. Nevertheless, during the first $\sim$ 1.3 fs, the values of $|S_{A'A''}(t)|$ remain sufficiently close to 1 to ensure approximate electronic coherence. This means that the present FC-excited superposition

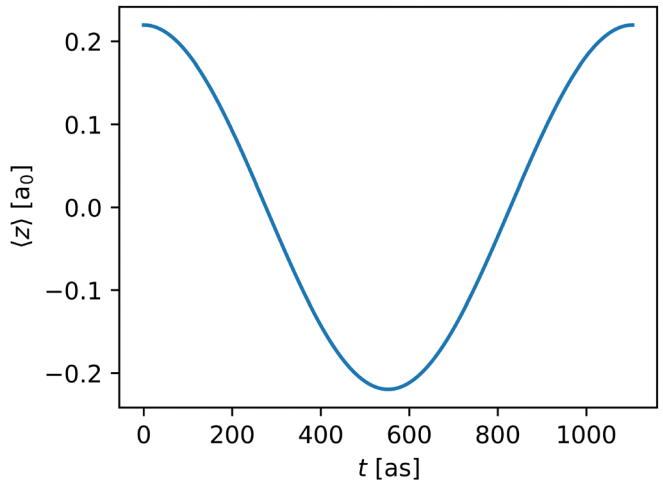

Fig. 3 Evolution of the chirality, measured as the expectation value of the out-of-plane coordinate as a function of time, $\langle z\rangle(t) = \int\int\int z\rho(\boldsymbol{r},t)\mathrm{d}x\mathrm{d}y\mathrm{d}z$.

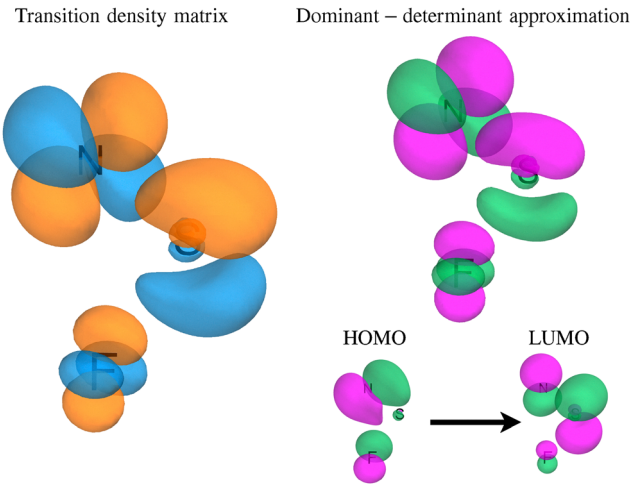

Fig. 4 Validity of the dominant-determinant approximation. Left: transition density matrix driving the attosecond chirality flip in eqn (19) obtained from the full many-electron wave packet. Positive/negative isocontours at $\pm 0.01/a_0{}^3$ in orange/blue. Right: transition density matrix (top) obtained from the dominant-determinant approximation, eqn (20). Positive/negative isocontours at $\pm 0.01/a_0{}^3$ in purple/green. The transition amounts approximately to a transition from HOMO to LUMO, which is depicted below. Positive/negative isocontours at $\pm 0.1/a_0{}^3$ in purple/green.

state $\psi(\boldsymbol{r},t;\mathbf{Q}_{\mathrm{m},A'})$ accounts for at least two electronic chirality flips, as illustrated in Fig. 2a/b.

Section S3 presents a detailed analysis of the rapid decay of $|S_{A'A''}(t)|$. In brief, after vertical $A' \rightarrow A''$ FC excitation of (part of) the vibrational ground state $\chi_{A',0}(\mathbf{Q})$, the nuclear wavepacket $\chi_{A''}(\mathbf{Q},t)$ on the excited uncoupled, adiabatic PES $V_{A''}(\mathbf{Q})$ rapidly departs from its initial state $\chi_{A'}(\mathbf{Q},0)$, which is centered at $\mathbf{Q}_{\mathrm{m},A'}$, and moves toward $\mathbf{Q}_{\mathrm{m},A''}$, the minimum of the excited-state PES. This causes rapid decay of the overlap $\langle\chi_{A''}(\mathbf{Q},0)|\langle\chi_{A''}(\mathbf{Q},t)\rangle$. Consequently, the rapid loss of electronic coherence—which limits the number of chirality flips of NSF in the superposition state $\psi(\mathbf{x},\mathbf{t};\mathbf{Q}_{\mathrm{m},A'})$—is primarily a consequence of the geometric shift from the potential minimum $\mathbf{Q}_{\mathrm{m},A'}$ to $\mathbf{Q}_{\mathrm{m},A''}$.

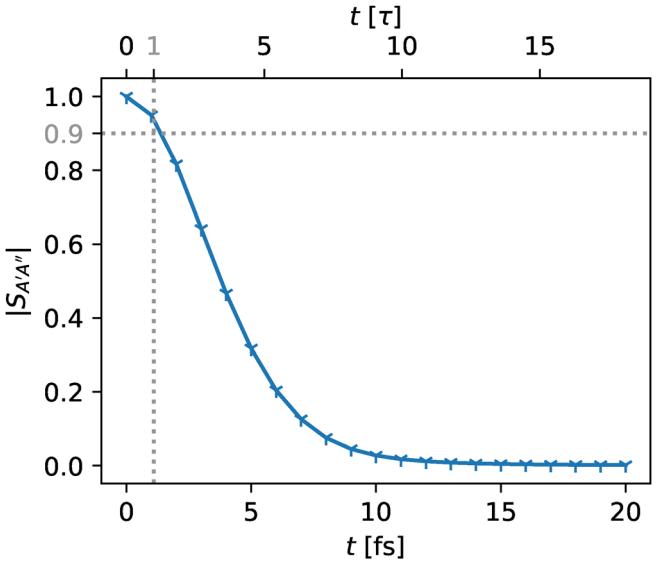

Fig. 5 Early-time evolution of the electronic coherences for a wave packet prepared in the $A' + A''$ electronic superposition state by FC excitation of NSF.

IV. Conclusions

The present FC-preparation of the electronic A'' superposition state of an oriented bent triatomic heteronuclear molecule is one of the easiest approaches, and most likely it is the easiest approach to electronic chirality flips in achiral molecules, in the time domain from a few hundred as to a few fs. This résumé rests on the requirement that all the symmetry elements which cause achirality in the electronic eigenstates of achiral molecules must be broken in the superposition state. Bent triatomic heteronuclear molecules are the smallest molecules which fulfill this requirement. They have only one, and it cannot be less than one, symmetry element which must be broken: the molecular symmetry plane σ. The superposition state consists of just two, and it cannot be less than two, constituting electronic eigenstates: the ground state A' plus a single excited state A''. Consequently, there is no simpler way than the present FC-preparation of the electronic $A' + A''$ superposition in the bent triatomic heteronuclear molecule, exemplified by NSF, to break the original symmetry—here C_s—down to C_1, which implies chirality.

One might suggest that this simple approach could also be applied to any planar molecules with more than three atoms. While this may be true for special cases, there is a counter-example: X-ray excitation of formic acid HCOOH to a superposition state of the electronic ground state plus a very highly excited state induces pyramidalization.[27] Consequently, the molecule which is achiral in the planar ground state is chiral in the pyramidal excited state. One can then no longer talk about electronic chirality in an achiral molecule. In contrast, triatomic heteronuclear molecules such as NSF cannot pyramidalize; they remain achiral as long as they are bent in both the electronic ground and excited states.

The present example NSF suffers from rapid electronic decoherence in the chiral $A' + A''$ superposition state. Consequently,

this allows only few chirality flips. The analysis in Section III shows that this disadvantage is mainly due to the shift of the minimum $\mathbf{Q}_{m,A'}$ of the potential energy surface $V_{A'}(\mathbf{Q})$ in the ground state A' to the different minimum $\mathbf{Q}_{m,A''}$ of $V_{A''}(\mathbf{Q})$ in the excited state A''. As an outlook, this suggests searching for bent triatomic heteronuclear molecules with near or, in the ideal case, perfectly coincident minima $\mathbf{Q}_{m,A'}$ and $\mathbf{Q}_{m,A''}$ of the PES in the electronic ground A' and excited A'' states. Such molecules should exhibit a much larger number of chirality flips in the $A' + A''$ superposition states, compared to NSF. Nevertheless, NSF will serve as a reference for the—most probably—simplest approach to electronic chirality flips in achiral molecules.

Conflicts of interest

There are no conflicts to declare.

Data availability

The supporting data has been provided as part of the supplementary information (SI). Supplementary information: Tables S1–S4 contain the relevant results from quantum chemistry calculations. Tables S5–S6 provide the information for reproducing the nuclear dynamics simulations. See DOI: https://doi.org/10.1039/d5cp04637h.

Acknowledgements

This work is dedicated to Professor N. Sathymurthy on the occasion of his 75th birthday. J. Manz expresses his gratitude for 4 decades of friendship in science. The Zentraleinrichtung für Datenverarbeitung (ZEDAT) of the Freie Universität Berlin is acknowledged for supplying computational resources.[28] J. Scherlitzki is grateful for the funding by the Elsa-Neumann scholarship of the federal state Berlin, Germany. Funding by the Deutsche Forschungsgemeinschaft (DFG, German Research Foundation) – Project-ID 387284271 – SFB 1349 is acknowledged.

Notes and references

1 A. Schönhofer, *Über die Beziehung zwischen den Symmetrien von Kern- und Elektronensystem einer Molekel*, [On the relationship between the symmetries of nuclear and electron system of a molecule], *Habilitation thesis*, Freie Universität Berlin, 1968.
2 V. Wanie, E. Bloch, E. P. Månsson, L. Colaizzi, S. Ryabchuk, K. Sarawathula, A. E. Ordonez, D. Ayuso, O. Smirnova and A. Trabattoni, *et al.*, *Nature*, 2024, **630**, 109.
3 M. Han, J.-B. Ji, A. Blech, R. E. Goetz, C. Allison, L. Greenman, C. P. Koch and H. J. Wörner, *Nature*, 2025, **645**, 95–100.
4 Y. Chen, D. Haase, J. Manz, H. Wang and Y. Yang, *Nat. Commun.*, 2024, **15**, 565.
5 C. Liu, J. Manz, H. Wang and Y. Yang, *Chem. Phys. Chem.*, 2025, **25**, e202400595.
6 T. Moitra, L. Konecny, M. Kadek, O. Neufeld, A. Rubio and M. Repisky, *J. Phys. Chem. Lett.*, 2024, **16**, 9210.
7 D. Haase, J. Manz and J. C. Tremblay, *J. Phys. Chem. A*, 2020, **124**, 3329.
8 D. Haase, G. Hermann, J. Manz, V. Pohl and J. C. Tremblay, *Symmetry*, 2021, **13**, 205.
9 O. Glemser and R. Mews, *Angew. Chem., Int. Ed. Engl.*, 1980, **19**, 883.
10 K. Kitano, N. Ishii and J. Itatani, *Phys. Rev. A:At., Mol., Opt. Phys.*, 2011, **84**, 053408.
11 L. Holmegaard, J. H. Nielsen, I. Nevo, H. Stapelfeldt, F. Filsinger, J. Küpper and G. Meijer, *Phys. Rev. Lett.*, 2009, **102**, 023001.
12 J. H. Nielsen, H. Stapelfeldt, J. Küpper, B. Friedrich, J. J. Omiste and R. González-Férez, *Phys. Rev. Lett.*, 2012, **108**, 193001.
13 P. M. Kraus, B. Mignolet, D. Baykusheva, A. Rupenyan, L. Horný, E. F. Penka, G. Grassi, O. I. Tolstikhin, J. Schneider and F. Jensen, *et al.*, *Science*, 2015, **350**, 790–795.
14 H.-J. Werner, P. J. Knowles, F. R. Manby, J. A. Black, K. Doll, A. Heßelmann, D. Kats, A. Köhn, T. Korona and D. Kreplin, *et al.*, *J. Chem. Phys.*, 2020, **52**, 144107.
15 J. Olsen and P. Jørgensen, *J. Chem. Phys.*, 1985, **82**, 3235–3264.
16 E. Dalgaard, *J. Chem. Phys.*, 1980, **72**, 816–823.
17 H.-J. Werner and W. Meyer, *J. Chem. Phys.*, 1981, **74**, 5794–5801.
18 T. H. Dunning Jr, K. A. Peterson and A. K. Wilson, *J. Chem. Phys.*, 2001, **114**, 9244–9253.
19 M. H. Beck, A. Jäckle, G. A. Worth and H.-D. Meyer, *Phys. Rep.*, 2000, **324**, 1–105.
20 G. Hermann, V. Pohl, J. C. Tremblay, B. Paulus, H.-C. Hege and A. Schild, *J. Comput. Chem.*, 2016, **37**, 1511–1520.
21 V. Pohl, G. Hermann and J. C. Tremblay, *J. Comput. Chem.*, 2017, **38**, 1515–1527.
22 A. D. Bandrauk, S. Chelkowski, P. B. Corkum, J. Manz and G. L. Yudin, *J. Phys. B: At., Mol. Opt. Phys.*, 2009, **42**, 134001.
23 C. Arnold, O. Vendrell and R. Santra, *Phys. Rev. A*, 2017, **95**, 033425.
24 H.-D. Meyer, U. Manthe and L. S. Cederbaum, *Chem. Phys. Lett.*, 1990, **165**, 73–78.
25 B. Hartke, R. Kosloff and S. Ruhman, *Chem. Phys. Lett.*, 1989, **158**, 238–244.
26 D. Jia, J. Manz, B. Paulus, V. Pohl, J. C. Tremblay and Y. Yang, *Chem. Phys.*, 2017, **482**, 146–159.
27 D. Tsitsonis, F. Trinter, J. B. Williams, K. Fehre, P. V. Demekhin, T. Jahnke, R. Dörner and M. S. Schöffler, *Phys. Rev. Lett.*, 2024, **133**, 093002.
28 L. Bennett, B. Melchers and B. Proppe, *Curta: A General-purpose High-Performance Computer at ZEDAT*, 2020, Freie Universität Berlin, https://refubium.fu-berlin.de/handle/fub188/26993.

